Online ISSN 1848-3380, Print ISSN 0005-1144
ATKAFF 55(4), 463–473(2014)

Károly Széll, András Czmerk, Péter Korondi

Friction with Hysteresis Loop Modeled by Tensor Product

DOI 10.7305/automatika.2014.12.628
UDK 681.511.4:629.064.2-586; 519.876.2
IFAC 4.3.2.3; 2.8

Original scientific paper

Engineers encounter the problem of friction in any mechanical system. Friction force is strongly nonlinear and varies considerably while the system is working. In the case of high-precision applications friction makes the situation even more complex, as the stick-slip effect occurs near the target position. This paper introduces a pneumatic servo-system for investigation of the behavior of friction near the target position. A new model is proposed which takes the hysteresis loop of the friction also into consideration emphasizing the importance of hysteresis. This paper presents the tensorproduct (TP) based modeling of friction which is suitable for control design. The main advantage of the TP model transformation is that due to its polytopic model form Linear Matrix Inequality (LMI) can be immediately applied to the resulting model to yield controllers with guaranteed performance. The main contribution of this paper is the application of TP model transformation making the identification of friction parameters unnecessary by utilizing directly the measured data itself.

Key words: Tensor Product, Friction Compensation, Pneumatic Cylinder, Stribeck Effect

Identifikacija modela trenja s histerezom korištenjem tenzorskog produkta. Inženjeri se susreću s pojavom trenja u svakom mehaničkom sustavu. Sila trenja ima izraženu nelinearnost i promjenjiva je ovisno o radnim uvjetima procesa. U slučaju pozicioniranja s visokom preciznošću trenje dodatno komplicira situaciju, što rezultira pojavom oscilatornog ponašanja u okolini referentne pozicije sustava upravljanja. U ovom radu je predstavljen pneumatski servosustav koji se koristi za analizu ponašanja sile trenja u blizini referentne pozicije. Predložen je novi model sile trenja koji uzima u obzir histereznu karakteristiku trenja. U radu je predstavljeno modeliranje trenja na principu tenzorskog produkta koji je prikladan za sintezu sustava upravljanja. Glavna prednost transformacije modela korištenjem tenzorskog produkta je što politopski oblik modela u obliku linearnih matričnih nejednadžbi omogućava njegovu direktnu primjenu za sintezu regulatora s garantiranim performansama. Glavni znanstveni doprinos ovog rada je primjena transformacije modela trenja korištenjem tenzorskog produkta, pri čemu identifikacija parametara trenja postaje suvišna direktnim korištenjem izmjerenih podataka.

Ključne riječi: tenzorski produkt, kompenzacija trenja, pneumatski cilindar, Stribeckov efekt

1 INTRODUCTION

Pneumatic actuators are widely used in industrial field due to their advantages like low cost, durability, high power-to-weight ratio etc. However their modeling and controlling is really challenging as they are strongly nonlinear: nonlinear overlapping of valve sections, air compressibility, heat transfer etc. One of the most interesting amongst these nonlinearities is the friction phenomenon.

Friction is omnipresent and a constant issue in any mechanical system [1-2]. In high precision applications for instance this can be a very annoying issue. Positioning can become really challenging. A proper model for friction could provide relief. However the very mechanisms of friction are still not fully understood and accurately modeled. Simple linear friction models do not perform well in solving this problem. Nonlinear approaches have also been proposed [3-5] with more or less success, many of them being based on empirically collected data. In this paper a novel approach is presented, based on tensor product (TP) transformation. The tensor product model form is a dynamic model representation whereupon Linear Matrix Inequality (LMI) based control design techniques [6-8] can immediately be executed. It describes a class of Linear Parameter Varying (LPV) models by the convex combination of linear time invariant (LTI) models, where the convex combination is defined by the weighting functions of each parameter separately. The TP model transformation is a recently proposed numerical method to transform LPV models into TP model form [9-11]. An important advantage of the TP model forms is that the convex hull of

the given dynamic LPV model can be determined and analyzed by one variable weighting functions. Furthermore, the feasibility of the LMIs can be considerably relaxed in this representation via modifying the convex hull of the LPV model.

Lots of theoretical models have been elaborated using TP during the last decade, however few applications have been practically implemented yet using TP transformations. This paper is intended to constitute a bridge between the mathematical description and the engineering applications.

The paper has the following structure. The next section introduces the mathematical framework of the TP transformation, then section 3 briefly presents different friction models, section 4 gives a description of the experimental setup, then section 5 introduces the tested models and section 6 gives a comparison of the simulation results.

2 THEORETICAL BACKGROUND OF THE TP TRANSFORMATION

Consider a parametrically varying dynamical system [1]:

$$\begin{array}{l} \dot{\mathbf{x}}(t) = \mathbf{A}(\mathbf{p}(t))\mathbf{x}(t) + \mathbf{B}(\mathbf{p}(t))\mathbf{u}(t) \\ \mathbf{y}(t) = \mathbf{C}(\mathbf{p}(t))\mathbf{x}(t) + \mathbf{D}(\mathbf{p}(t))\mathbf{u}(t) \end{array}, \tag{1}$$

with input $\mathbf{u}(t) \in \mathbb{R}^p$, output $\mathbf{y}(t) \in \mathbb{R}^q$ and state vector $\mathbf{x}(t) \in \mathbb{R}^n$. The system matrix is a parameter-varying object, where $_{|}(t) \in \Omega$ is a time varying N-dimensional parameter vector, and is an element of the closed hypercube $\mathbf{\Omega} = [a_1, b_1] \times [a_2, b_2] \times \ldots \times [a_N, b_N] \in \mathbb{R}^N$. The parameter $\mathbf{p}(t)$ can also include some elements of $\mathbf{x}(t)$.

Given the LPV system description in (1), it can be reformulated using:

$$\mathbf{S}(\mathbf{p}(t)) = \begin{pmatrix} \mathbf{A}(\mathbf{p}(t)) & \mathbf{B}(\mathbf{p}(t)) \\ \mathbf{C}(\mathbf{p}(t)) & \mathbf{D}(\mathbf{p}(t)) \end{pmatrix} \in \mathbb{R}^{(n+p)\times(n+q)}, \tag{2}$$

thus:

$$\begin{pmatrix} \dot{\mathbf{x}}(t) \\ \mathbf{y}(t) \end{pmatrix} = \mathbf{S}(\mathbf{p}(t)) \begin{pmatrix} \mathbf{x}(t) \\ \mathbf{u}(t) \end{pmatrix}. \tag{3}$$

Expression (2) may be approximated over any **p**(*t*) using a number of *R* LTI system matrices ($\mathbf{S_r}$, *r*=1, ..., *R*). These $\mathbf{S_r}$ matrices are also known as LTI vertex models. The convex combination can be built using the weighting functions $\mathrm{w}_r(\mathbf{p}(t)) \in [0, 1]$ in such manner, that $\mathbf{S}(\mathbf{p}(t))$ fits into the convex hull formed by $\mathbf{S_r}$, that is $\mathbf{S}(\mathbf{p}(t)) = co\{\mathbf{S_1}, \mathbf{S_2}, ..., \mathbf{S_R}\}_{\mathrm{w}(\mathbf{p}(t))}$. The explicit form of the tensor product then becomes:

$$\begin{pmatrix} \dot{\mathbf{x}}(t) \\ \mathbf{y}(t) \end{pmatrix} \approx \left(\sum_{i_1=1}^{I_1} \sum_{i_2=2}^{I_2} \cdots \sum_{i_N=1}^{I_N} \prod_{n=1}^{N} \mathrm{w}_{n,i_n} \cdots (p_n(t))\mathbf{S}_{i_1,i_2,\ldots,i_N} \right) \begin{pmatrix} \mathbf{x}(t) \\ \mathbf{u}(t) \end{pmatrix}. \tag{4}$$

The function $\mathrm{w}_{n,j}(p_n(t))$ is the j^{th} basis function belonging to the n^{th} dimension of $\mathbf{\Omega}$ and $p_n(t)$ is the n^{th} element of the $\mathbf{p}(t)$ vector. I_n denotes the number of weighting functions used in the n^{th} dimension. The multiple indexes $i_1, i_2, ..., i_N$ point at the LTI system associated with the ${i_n}^{th}$ weighting function. There are $R = \prod^N I_N$ LTI systems denoted $\mathbf{S}_{i_1,i_2,\ldots,i_N}$.

TP model to be a convex combination, the weighting functions must satisfy:

$$\forall n, p_n : \sum_{i=1}^{I_n} w_{n,i}(p_n) = 1. \tag{5}$$

The main steps of the Tensor Product Model Transformation as shown in Fig. 1. are:

- first we need a discretized model in $\mathbf{p} \in \Omega$. As shown in Fig. 1, the discretized model can be obtained from measurement in direct way or using a nonlinear analytical $\mathbf{S}(\mathbf{p}(t))$ model and the computation of system matrix $\mathbf{S}(\mathbf{g})$ over the grid points $\mathbf{g}$ of a hyperrectangular grid net defined in Ω.
- the second step extracts the singular value based orthonormal structure of the system, namely, this step determines the minimal number the LTI systems in orthonormal position according to the ordering of the singular values and defines the orthonormal discretized weighting functions of the searched polytopic model.
- the LTI systems and the discretized weighting functions can be modified, in order to satisfy further conditions for the weighting functions: for instance, this step can ensure the convexity of the weighting functions (5).

3 FRICTION MODELS OVERVIEW

This overview is neither intended to be exhaustive nor detailed. It is only to briefly review some of the most widely applied friction models.

Probably the most simple and most straightforward way of modeling friction is to assume friction is constant and opposite to the direction of motion (see Fig. 2a). This makes friction independent from the value of the velocity and size of the contact area:

$$F_{Fr} = F_c \mathrm{sign}(v), \tag{6}$$

where F_c friction force is proportional to the normal load:

$$F_c = \mu F_N. \tag{7}$$

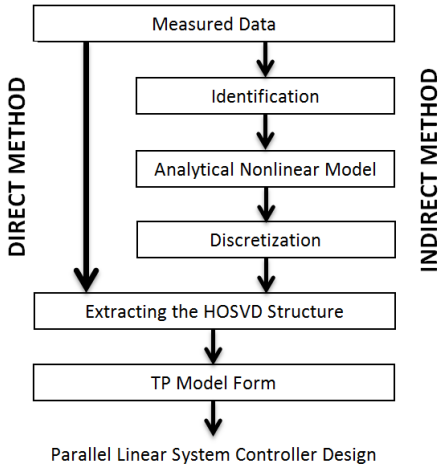

Fig. 1. TP transformation based design algorithm

This is the Coulomb friction model.

One of the main shortcomings of the Coulomb model is the absence of zero velocity friction force, which in reality is very present. Also the independence from the velocity is contrary to what has been experienced with real systems. To overcome these issues, the Coulomb model can be completed for instance with the viscous friction model which states:

$$F_{Fr} = F_v v. \tag{8}$$

The model is used for the friction caused by the viscosity of the fluids, specifically lubricants. A combination with Coulomb friction yields (see Fig. 2b):

$$F_{Fr} = F_c \text{sign}(v) + F_v v. \tag{9}$$

The model can be refined by adding the influence of an external force for the friction at rest. This, however, leads to a discontinuous function. Here, an important contribution has been made by Stribeck, who proposed a model which involves a nonlinear, but continuous function:

$$F_{Fr}(v) = \left(F_C + (F_s - F_C) \cdot e^{-\left|\frac{v}{v_s}\right|^\delta}\right) \text{sign}(v) + F_v \cdot v, \tag{10}$$

where v_s is the Stribeck velocity, δ is an empirical parameter, F_s is the static friction force. A similar model was employed by Hess and Soom [12].

$$F_{Fr}(v) = \left(F_C + \frac{(F_s - F_C)}{1 + (v/v_s)^2}\right) \text{sign}(v) + F_v v \tag{11}$$

The Stribeck curve is an advanced model of friction as a function of velocity (see Fig. 2d). Although it is still valid only in steady state, it includes the model of Coulomb, static and viscous friction as built-in elements. There are several more advanced models in the technical literature [13-15]. This paper does not intend to introduce any new friction model. Only a new representation of the existing models is proposed which is suitable for controller design. The main contribution of this new model is that the effect of the hysteresis is applied in the simulation and the model is constructed in a way that can be handled by controller design algorithms suitable for nonlinear systems.

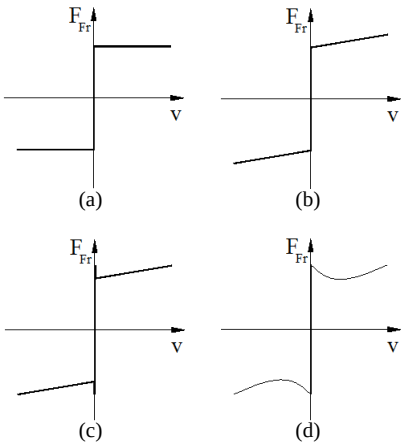

Fig. 2. Different friction curves (friction vs. velocity): a) Coulomb friction, b) viscous friction, c) influence of an external force for the friction at rest added to the viscous friction, d) Stribeck curve

4 SYSTEM DESCRIPTION

4.1 Servo-pneumatic system

The control of pneumatic systems can be very challenging, due to their strong nonlinearity [16-20]. As a first step of control design in this paper we focus on the modeling of our experimental setup. The case is complex, as there is nonlinear correlation between the volume flow and chamber pressure, nonlinear overlapping of valve sections, air compressibility, heat transfer on the chamber wall etc.

The question is which effect is worth modeling. If we carry out a deeper investigation of the system it can be highlighted that influence of the thermal effects is minimal. The behavior of the servo-pneumatic system depends on electronic, mechanic, fluid and thermal effects. Comparing these effects we can see that the time constant of the thermal phenomenon is at least one order of magnitude higher, thus the heat transfer has no significant influence on the dynamic behavior of the pneumatic system. As our modeling focuses on the phenomenon of friction we neglected the thermal and air leakage effects. Based on the above considerations our model is handled as adiabatic, reversible, thus an isentropic process.

The mechanical part of the pneumatic system can be interpreted as a simple spring-mass system, where the chamber volumes act like springs and pressure gives the spring stiffness. This stiffness is relatively small for pneumatic systems. Friction appears between the piston and the chamber-wall and between the piston-rod and the cylinder-cover. It has a strong influence in the case of pneumatic systems during position control due to the previously mentioned facts. Thus the effect of stick-slip can be investigated much easier.

Nomenclature for the experimental setup:

A - surface of the piston

V_0 - dead volume at the end of the piston

l - stroke length

κ - heat coefficient ratio

R - specific gas constant of air

T - chamber temperature

α - flow rate coefficient of form

A_v - flow surface of the valve

ψ - flow rate coefficient of pressure difference

p_a - pressure of the left chamber

p_b - pressure of the right chamber

p_n - pressure of upstream flow

p_m - pressure of downstream flow

p_S - supply pressure

p_E - exhaust pressure

F_{fr} - friction force

x - piston position

v - piston velocity

$\dot{m}_i$ - mass flow

The dynamics of the piston depend on the chamber pressures, which can be changed basically by two processes: airflow inwards and airflow outwards.

$$m \cdot \dot{v} - p_a \cdot A + p_b \cdot A + F_{Fr} = 0 \tag{12}$$

The pressure built up in the cylinder during isentropic process is described by the following differential equation for the left chamber side:

$$\dot{p}_a \cdot (V_0 + A \cdot x) = \kappa \cdot (R \cdot T \cdot \dot{m}_a - A \cdot \dot{x} \cdot p_a), \tag{13}$$

respectively for the right chamber side:

$$\dot{p}_b \cdot (V_0 + A \cdot (l - x)) = \kappa \cdot (R \cdot T \cdot \dot{m}_b + A \cdot \dot{x} \cdot p_b). \tag{14}$$

The mass flows based on Fig. 3.:

$$\dot{m}_a = \dot{m}_2 - \dot{m}_1, \tag{15}$$

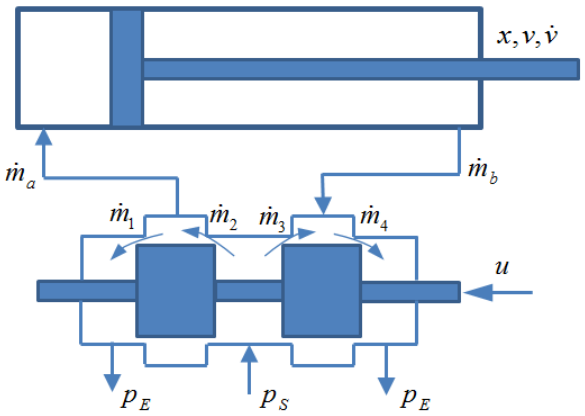

Fig. 3. Schematic mass flow diagram of cylinder and valve

$$\dot{m}_b = \dot{m}_4 - \dot{m}_3. \tag{16}$$

Let us build up a state space for our experimental setup. The state variables are the piston position *x*, the piston velocity *v*, the pressure of the left chamber *pa* and the pressure of the right chamber *pb*, the control signal *u* is the control voltage of the valve.

$$\begin{pmatrix} \dot{x} \\ \dot{v} \\ \dot{p}_a \\ \dot{p}_b \end{pmatrix} = \begin{pmatrix} 0 & 1 & 0 & 0 \\ 0 & a_{22} & \frac{A}{m} & -\frac{A}{m} \\ 0 & a_{32} & 0 & 0 \\ 0 & a_{42} & 0 & 0 \end{pmatrix} \begin{pmatrix} x \\ v \\ p_a \\ p_b \end{pmatrix} + \ldots$$
$$\ldots + \begin{pmatrix} 0 \\ 0 \\ b_{31} \\ b_{41} \end{pmatrix} u, \tag{17}$$

where:

$$a_{22}(v) = -\frac{F_{Fr}(v)}{v \cdot m}, \tag{18}$$

$$a_{32}(x, p_a) = -\frac{A \cdot p_a}{V_0 + A \cdot x}, \tag{19}$$

$$a_{42}(x, p_b) = \frac{A \cdot p_b}{V_0 + A \cdot (l - x)}, \tag{20}$$

$$b_{31}(x, p_a) = \frac{\kappa \cdot R \cdot T}{V_0 + A \cdot x} \cdot \ldots$$
$$\ldots \cdot \alpha \cdot A_v \cdot \psi\left(\frac{p_n}{p_m}\right) \cdot p_n \cdot \sqrt{\frac{2}{R \cdot T}}, \tag{21}$$

$$b_{41}(x, p_b) = -\frac{\kappa \cdot R \cdot T}{V_0 + A \cdot (l - x)} \cdot \ldots$$
$$\ldots \cdot \alpha \cdot A_v \cdot \psi\left(\frac{p_n}{p_m}\right) \cdot p_n \cdot \sqrt{\frac{2}{R \cdot T}}. \tag{22}$$

4.2 Measurement of friction with hysteresis loop

This paper concentrates on the description of the friction F_{Fr}, thus on the definition of a_{22}. For this purpose

an experimental setup was built focusing on the stick-slip effect. The experimental setup can be seen in Fig. 4. The experiments are carried out on a standard DSNU-20-100-PPV-A Festo pneumatic cylinder equipped with a 5/3 proportional magnet valve, two pressure sensors and an accelerometer.

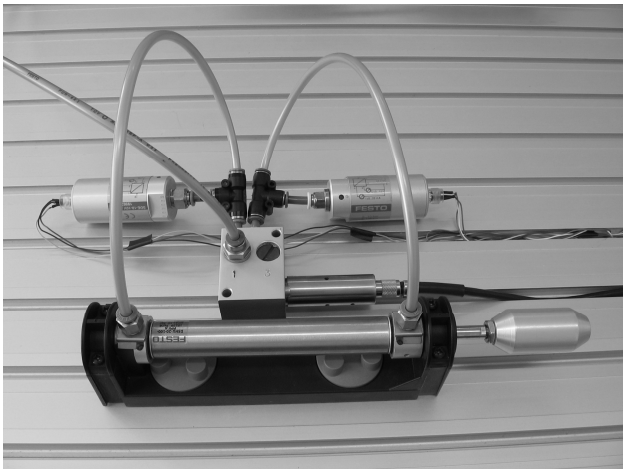

Fig. 4. Experimental setup

The identification of friction is based on the investigation of the stick-slip effect. As mentioned before, this effect might be much stronger in the case of pneumatic cylinders, making the identification of the friction force easier.

As excitation we set a fix voltage on the magnet valve, in other words we started to load the left chamber with slowly rising pressure while the right chamber was exhausted. In Fig. 5. we can see the pressure difference of the two chambers during our experimental measurement which gives us the force acting on the piston.

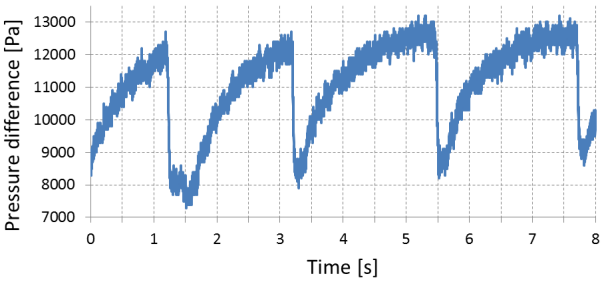

Fig. 5. Excitation

As we can see, when the excitation force reaches the value of the static friction, the piston starts to move (slip), which motion rapidly increases the volume of the left chamber. Due to the increasing volume the pressure of the left chamber drops, resulting low pressure difference. Thus the excitation force will also drop, the piston starts to slow down, and at the end it will reach its new steady state (stick).

As the excitation voltage is continuously at the same voltage level, at steady state the pressure will start to increase again. Thus the process starts from the beginning with the slipping of the piston at an excitation force stepping over the static friction. This way measurements can be taken right in the area of the friction hyteresis.

In Fig. 6. and 7. one single stick-slip process is cut from the measurement, showing the measured pressure difference of the chambers and the measured acceleration.

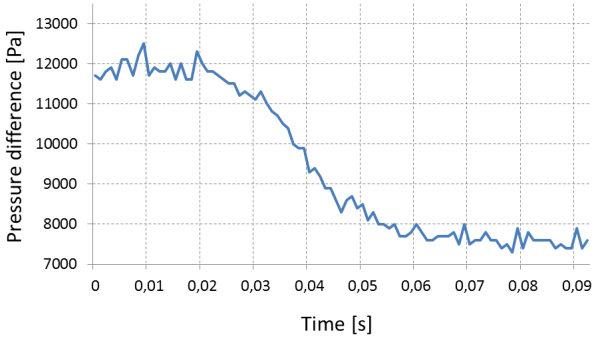

Fig. 6. Excitation for a single Stick-Slip

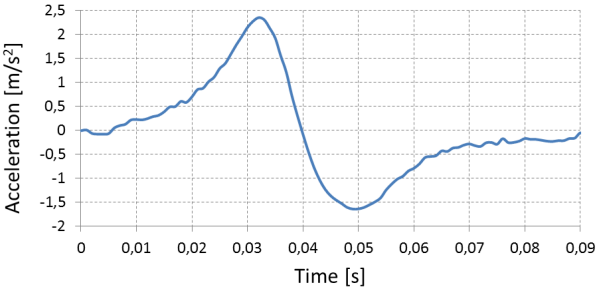

Fig. 7. Acceleration during Stick-Slip

Based on the measured acceleration we can calculate the velocity by integration. Figure 8. shows the velocity-profile during slip-stick.

We know the mass and the acceleration of the piston. Thus we know the force needed for the motion. Based on the measured pressures we indirectly measured the force acting on the piston. The difference of these two forces was dissipated by the friction. Thus we have the friction force as the function of velocity (see Fig. 9.).

The next section gives us an overview of the applied models and the parameters of the friction models.

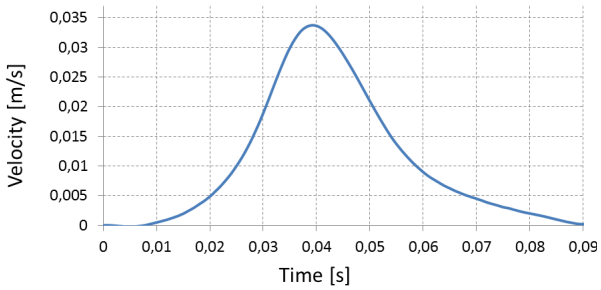

Fig. 8. Velocity during Stick-Slip

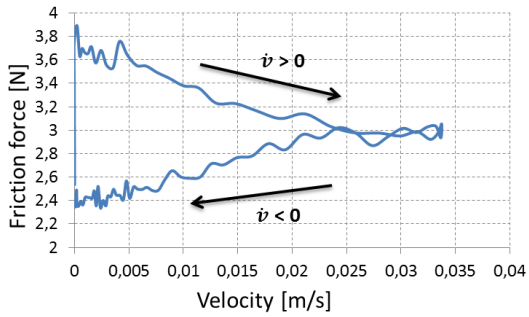

Fig. 9. Stribeck hysteresis

5 MODEL FORMULATION

Four different friction models were derived to make a comparison based on the measurements:

- MODEL A:
  Nonlinear parametric model based on (11) without hysteresis (conventional model based on literature).
- MODEL B:
  Nonlinear parametric model based on (11) with the newly proposed hysteresis model.
- MODEL C:
  TP model derived via indirect method of TP transformation (see Fig. 1.) based on nonlinear parametric model with hysteresis loop.
- MODEL D:
  TP model derived via direct method of TP transformation (see Fig. 1.) directly applying the measurement results of the experiments.

5.1 Model A

Based on the friction model (11) proposed by the literature, the identification of the parameters has given the following result:

$$F_C = 2.447 \text{ [N]},$$
$$F_S = 3.7 \text{ [N]},$$
$$F_v = 15 \text{ [Ns/m]},$$
$$v_s = 0.019 \text{ [m/s]}.$$

Model A describes only the Stribeck curve with no hysteresis, thus the friction force is the same for acceleration and for braking situation (see Fig. 10.).

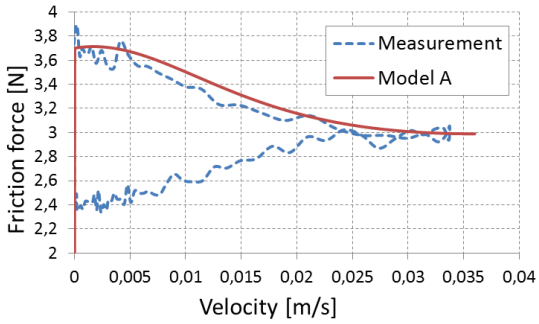

Fig. 10. Stribeck hysteresis for Model A

5.2 Model B

In the case of the second model a new approach is proposed where we use the friction models (9) and (11), based on the sign of the acceleration:

$$F_{Fr}(v) = \begin{cases} \left(F_C + \frac{(F_s - F_C)}{1+(v/v_s)^2}\right)\text{sign}(v) + F_v v, \text{ if } \dot{v} \geq 0 \\ F_c \text{sign}(v) + F_v v, \text{ if } \dot{v} < 0 \end{cases} \quad (23)$$

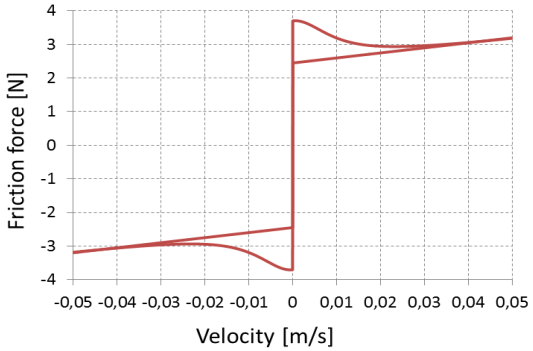

Fig. 11. Simulated Stribeck curve

Figure 11. shows the simulated Stribeck curve with hysteresis. In Fig. 12. the hysteresis loop is emphasized distinguishing the acceleration and braking situation.

Model B gives the following friction hysteresis compared to the measurement results:

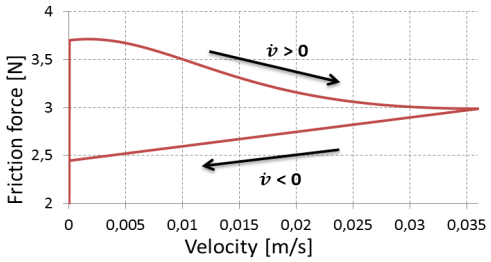

Fig. 12. Simulated Stribeck curve

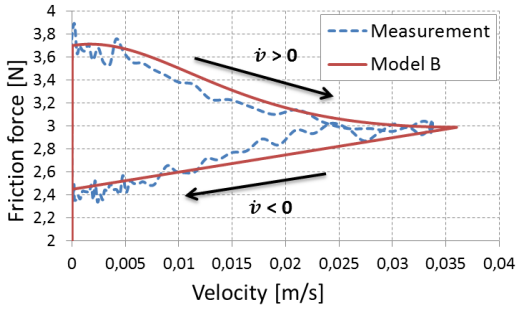

Fig. 13. Stribeck hysteresis for Model B

The model is built up using parametric equations. The main contribution of this model is the hysteresis loop in the friction.

5.3 Model C

The third model was designed using the indirect method of TP transformation (see Fig. 1.) based on (23). The operation area of our experiment defines the domain and grid size of the discretization process for TP transformation. Thus the domain for the velocity is between -0.05 and 0.05 m/s with a grid size 1000 which takes 1000 discrete values in the defined domain. To specify the hysteresis loop, the TP transformation was applied for both parametric equation (9) and (11). (11) is denoted by Str and (9) is denoted by Vis.

After applying the TP transformation, the friction for accelerated piston can be modeled using the following linear combination:

$$a_{22}^{Str1} = -7.25 \cdot 10^5, \tag{24}$$

$$a_{22}^{Str2} = -590, \tag{25}$$

where the weighting as the function of the velocity:

After applying the TP transformation, the friction for slowing piston can be modeled using the following linear combination:

$$a_{22}^{Vis1} = -4.79 \cdot 10^5, \tag{26}$$

$$a_{22}^{Vis2} = -590, \tag{27}$$

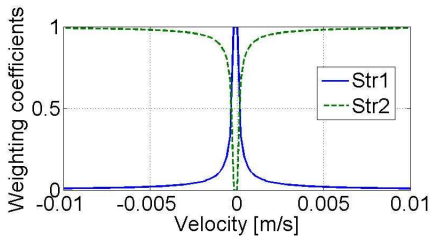

Fig. 14. The weighing coefficients as function of velocity for Model C

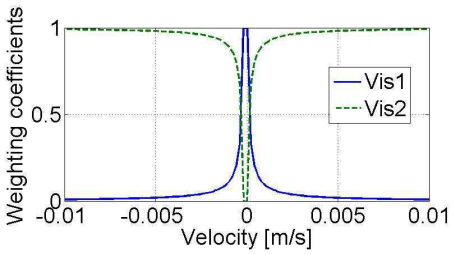

Fig. 15. The weighing coefficients as function of velocity for Model C

where the weighting as the function of the velocity:

The shape of the functions is quite straightforward to explain. The nonlinear friction terms are modeled using a varying viscosity coefficient, which is represented by the a_{22} element in the system matrix. A small viscous coefficient in a_{22}^2 dominates at high speed, where the Coulomb friction is relatively small. A very large viscous coefficient in a_{22}^1 dominates at low speed, where the Coulomb friction is comparatively large. We can also see that the rate of a_{22}^{Str1} and a_{22}^{Vis1} gives us the rate of F_S and F_C.

Model C gives the following friction hysteresis:

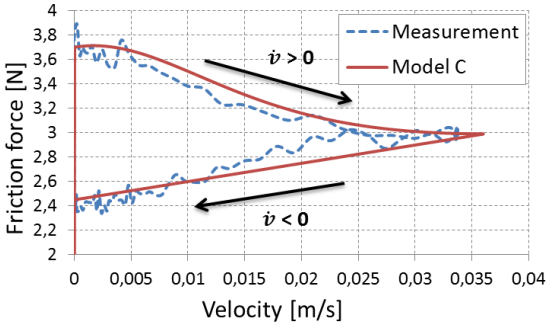

Fig. 16. Stribeck hysteresis for Model C

As we can see the model gives a good approximation of the measurement results.

5.4 Model D

The fourth model was designed using the direct method of TP transformation (see Fig. 1.). The same domain and grid size was applied as in the case of Model C but for data input instead of a parametric equation directly the measurement data was used.

After applying the TP transformation, the friction for accelerated piston can be modeled using the following linear combination:

$$a_{22}^{Str1} = -4.21 \cdot 10^4, \tag{28}$$

$$a_{22}^{Str2} = -598, \tag{29}$$

where the weighting as the function of the velocity:

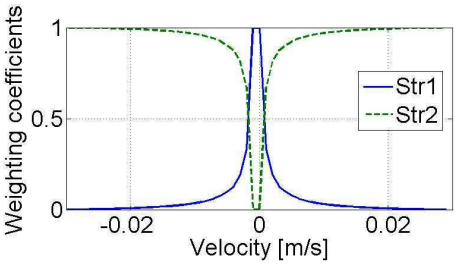

Fig. 17. The weighing coefficients as function of velocity for Model D

After applying the TP transformation, the friction for slowing piston can be modeled using the following linear combination:

$$a_{22}^{Vis1} = -2.76 \cdot 10^4, \tag{30}$$

$$a_{22}^{Vis2} = -598, \tag{31}$$

where the weighting as the function of the velocity:

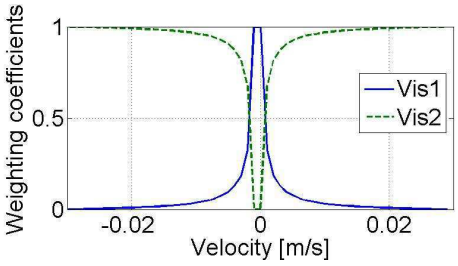

Fig. 18. The weighing coefficients as function of velocity for Model D

The friction hysteresis of Model D is shown in Fig. 19. Note that Model D has almost the same friction hysteresis as derived from the measurement. In Fig. 19. they are overlapping each other. The difference depends on the grid size of the TP transformation. The more measurement data we use in the TP transformation process the smaller the difference will be. There are two advantages of Model D. One is that it is not necessary to identify the parameters of the friction model (23), but we can use directly our measurements. The second is that we created a model suitable for TP control design, which provides already implemented control design tools for nonlinear systems.

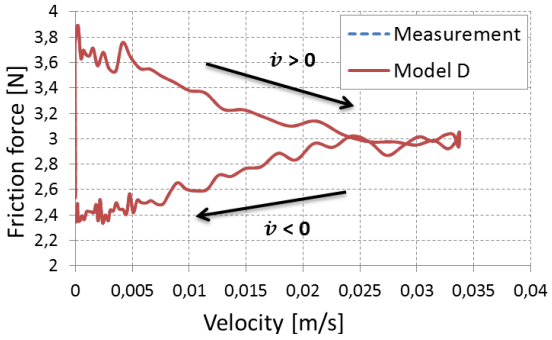

Fig. 19. Stribeck hysteresis for Model D

6 COMPARISON

The four models are compared by using the same excitation measured during a single stick-slip phenomenon (see Fig. 6.). Thus as excitation the pressure difference from the measurement is applied in every cases and the responses of the four models are investigated. The comparison is based on the investigation of the acceleration- and velocity-answers of the different models.

6.1 Deviation of the models

The comparison of the root-mean-square deviation (RMSD) of the models compared to the measurement can be seen in Table 1.

Table 1. RMSD of the models

Deviation	**Models**			
	Model A	***Model B***	***Model C***	***Model D***
Acceleration [m/s2]	0.959	0.1059	0.1062	0.1092
Acceleration [%]	24.04	2.654	2.661	2.736
Velocity [m/s]	0.00494	0.00183	0.00182	0.00238
Velocity [%]	14.54	5.372	5.340	7.013

In the case of Model A we can notice a significant difference between the simulation and the measurement. The

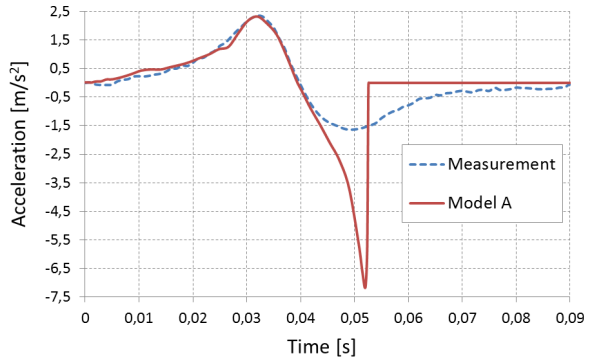

Fig. 20. Acceleration of Model A

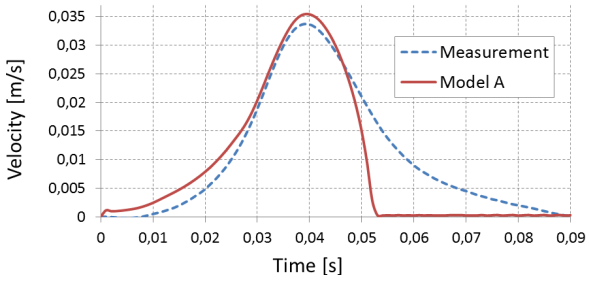

Fig. 21. Velocity of Model A

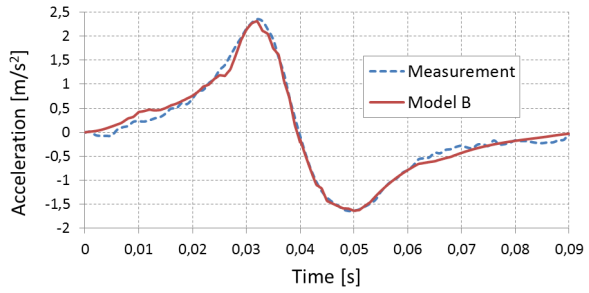

Fig. 22. Acceleration of Model B

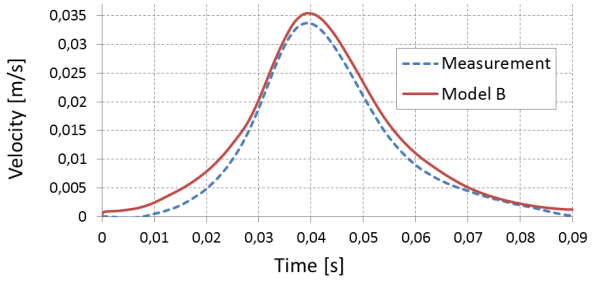

Fig. 23. Velocity of Model B

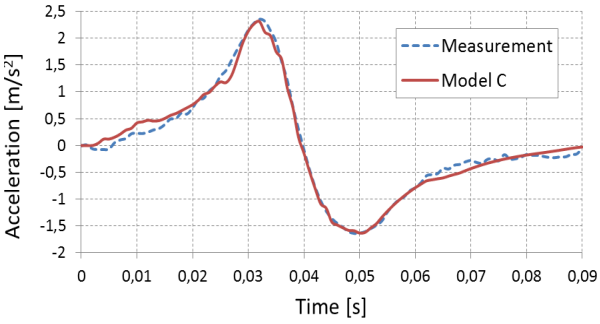

Fig. 24. Acceleration of Model C

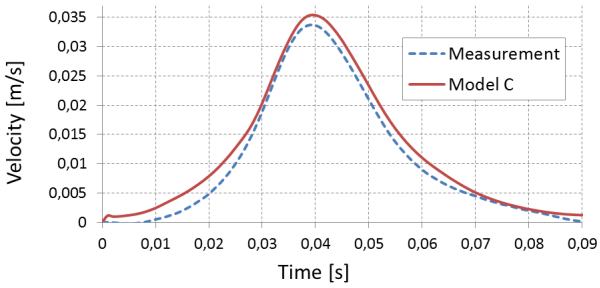

Fig. 25. Velocity of Model C

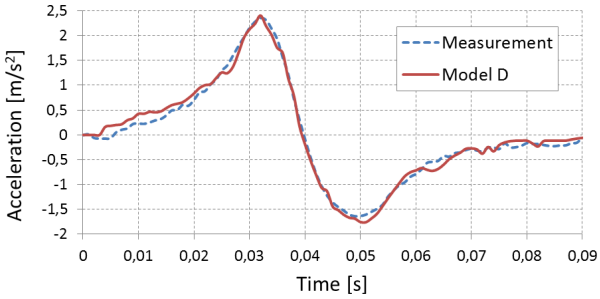

Fig. 26. Acceleration of Model D

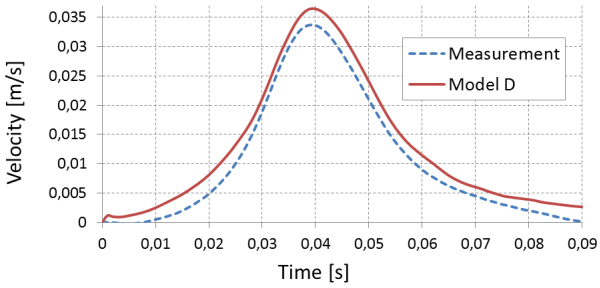

Fig. 27. Velocity of Model D

lack of hysteresis in the friction model based on the sign of acceleration highly influences the results of the stick-slip simulation.

The simulation of Model B gives a very good approximation of the measurement results due to the proposed hysteresis.

Model C is almost the same as Model B considering the friction model. This can also be noticed on the simulation results. The difference depends on the grid size of the TP transformation. The more discretized data we use in the TP transformation process the smaller the difference will be. The main advantage of Model C is that the algorithms of TP control design for nonlinear systems can be applied for it.

Model D gives us a bit bigger difference as it is designed using the measurement data directly with no filtering. Thus the noise collected by the sensors is also built in the model. This inaccuracy can be depressed using the statistical result of repeated measurements. There are two advantages of Model D. One is that it is not necessary to identify the parameters of the friction model, but the measurement data can be directly applied for modeling. The second is that Model D is suitable for TP control design, which provides already implemented control design tools for nonlinear systems.

7 CONCLUSION

In this paper friction with hysteresis loop was addressed, with a brief theoretical background of the mathematical framework, friction and pneumatic servo-system models. The results show dramatic improvement in the case of applying the hysteresis instead of the conventional model without hysteresis. The application of the TP transformation made it possible to omit the identification process, still granting its control design resources for nonlinear systems.

ACKNOWLEDGMENT

The authors wish to thank the support to the Hungarian Automotive Technicians Education Foundation, to the Hungarian Research Fund (OTKA K100951), and the Control Research Group of HAS. The results discussed above are supported by the grant TÁMOP-4.2.2.B-10/1–2010-0009.

REFERENCES

[1] P. Gróf, B. Takarics, Z. Petres, P. Korondi, “Tensor product model type polytopic decomposition of a pneumatic system with friction phenomena taken into account”, 8th IEEE International Symposium on Applied Machine Intelligence and Informatics, ISBN: 978-1-4244-6422-7, pp. 153-158., 2010.

[2] P. T. Zwierczyk, K. Váradi, “Frictional contact FE analysis in a railway wheel-rail contact”, Periodica Polytechnika Mechanical Engineering Vol 58 No 2, pp. 93– 99, 2014.

[3] Ante Božić, Joško Deur, Nedjeljko Perić, “Gain Scheduling-based Friction Compensation”, Proceedings of the 35th IEEE Industry Applications Conference, Roma, Italy, Vol.2, pp.1089-1095, 2000.

[4] Karim Khayati, Pascal Bigras, Louis-A. Dessaint, “LuGre model-based friction compensation and positioning control for a pneumatic actuator using multi-objective output-feedback control via LMI optimization”, Mechatronics 19, pp. 535–547, 2009.

[5] Zheng Chen, Bin Yao, Qingfeng Wang, “Adaptive Robust Precision Motion Control of Linear Motors With Integrated Compensation of Nonlinearities and Bearing Flexible Modes”, IEEE Transactions on Industrial Informatics, Vol. 9., pp. 965-973, 2013.

[6] S. Boyd, L. E. Ghaoui, E. Feron, and V. Balakrishnan, “Linear matrix inequalities in system and control theory,” Philadelphia PA:SIAM, ISBN 0-89871-334-X, 1994.

[7] P. Gahinet, A. Nemirovski, A. J. Laub, and M. Chilali, “LMI Control Toolbox”, The MathWorks Inc., 1995.

[8] C. W. Scherer and S. Weiland, “Linear Matrix Inequalities in Control”, ser. DISC course lecture notes, 2000.

[9] P. Galambos, P. Baranyi, P. Korondi,” Extended TP Model Transformation for Polytopic Representation of Impedance Model with Feedback Delay”, WSEAS Transactions on Systems and Control 5:(9), pp. 701-710., 2010.

[10] Z. Petres, P. Baranyi, P. Korondi, H. Hashimoto, ”Trajectory tracking by TP model transformation: case study of a benchmark problem”, IEEE Transactions on Industrial Electronics 54:(3), pp. 1654-1663., 2007.

[11] Lathauwer, L., Moor, B. and Vandewalle, J., “ A multilinear singular value decomposition”, SIAM Journal on Matrix Analysis and Applications, 21(4), pp. 1253-1278, 2000.

[12] Hess, D. P. and Soom, A., "Friction at a Lubricated Line Contact Operating at Oscillating Sliding Velocities," J. of Tribology 112(1), pp. 147-152., 1990.

[13] Rabinowicz, E., “Friction and Wear of Materials”, John Wiley and Sons, NY, 1995.

[14] Armstrong-Hélouvry, B., Dupont, P. and de Wit, C., “A Survey of Models, Analysis Tools and Compensation Methods for the Control of Machines with Friction”, Automatica 30(7), pp. 1083-1138., 1994.

[15] I.-C. Bogdan, G. Abba, “Identification of mechanical parameters at low velocities for a micropositioning stage using a velocity hysteresis model”, IEEE International Conference on Robotics and Automation (ICRA), pp. 430-435, 2012.

[16] András Czmerk, “Dynamics of a servopneumatic drive”, VII. International PhD Workshop. Gliwice, Poland, pp. 343-346., 2005.

[17] M. F. Rahmat, Sy Najib Sy Salim, N. H. Sunar, Ahmad ‘Athif Mohd Faudzi, Zool Hilmi Ismail and K. Huda, “Identification and non-linear control strategy for industrial pneumatic actuator”, International Journal of the Physical Sciences Vol. 7(17), pp. 2565 - 2579, 23 April, 2012.

[18] Sy Najib Sy Salim, M.F. Rahmat, A.M. Faudzi, N.H. Sunar, Z.H. Ismail, Sharatul Izah Samsudin, "Tracking performance and disturbance rejection of pneumatic actuator system", IEEE 978-1-4673-5769-2/13, 2013.

[19] Yung-Tien Liu, Tien-Tsai Kung, Kuo-Ming Chang, Sheng-Yuan Chen, "Observer-based adaptive sliding mode control for pneumatic servo system", Precision Engineering 37, pp. 522– 530, 2013.

[20] Cs. Hős, B. Kuti, "An experimental and theoretical study on the effect of sampling time delay on the stability of a PI position controller of a hydraulic cylinder", Periodica Polytechnika Mechanical Engineering Vol 57 No 2, pp. 23– 27, 2013.

Károly Széll received his MSc degree in Mechatronics at Budapest University of Technology and Economics. Currently, he is a PhD student in the Department of Mechatronics, Optics and Engineering Informatics. His interest area is control theory and sliding mode control.

András Czmerk received the MSc degree in mechanical engineering from the Technical University of Budapest, Hungary in 2003. Since 2008, he has been working as assistant lecturer in the Department of Mechatronics, Optics and Engineering Informatics. His research interests are modelling and position control of pneumatic systems.

Péter Korondi received the Dipl.Ing. and Ph.D. degrees in electrical engineering from the Technical University of Budapest (BME), Hungary, in 1984 and 1995, respectively. Since 1986, he has been with BME, where he is currently a professor in the Department of Mechatronics, Optics and Engineering Informatics. From April 1993 to April 1995, he worked in the Institute of Industrial Science, University of Tokyo, Japan. His current research interests include cognitive telemanipulation and etho-robotics. Author or co-author of 13 book chapters, university notes, 64 Hungarian and foreign journal papers, 161 conference papers (including 4 Keynote lectures), 12 R&D studies; held 34 presentations at foreign universities and institutes; 921 independent citations to his work. He was the general chair of ASME/IEEE Advanced Intelligent Mechatronics Conference in 2011. He is the chair of IEEE IES - Technical Committee on Control, Robotics & Mechatronics from 2011. He is the chair of IFAC - Technical Committee 4.3 on Robotics 2011. He is member of Control Engineering Research Group of the HAS at the Department of Automation.

AUTHORS' ADDRESSES

Károly Széll, M.Sc.
András Czmerk, M.Sc.
Prof. Péter Korondi, Ph.D
Department of Mechatronics, Optics and Engineering Informatics,
Faculty of Mechanical Engineering,
Budapest University of Technology and Economics,
1521 Budapest, Pf. 91., Hungary
email: szell, czmerk, korondi@mogi.bme.hu

Received: 2013-08-01
Accepted: 2014-08-25